



Application of nanoporous material MCM-41 in a membrane adsorption reactor (MAR) as a hybrid process for removal of methyl orange

Talib M. Albayati

*Department of Chemical Engineering, University of Technology, 52 Alsinaa St., PO Box 35010, Baghdad, Iraq,
email: talib_albyati@yahoo.com*

Received 11 October 2018; Accepted 27 January 2019

ABSTRACT

The hybrid systems have been proven to be the most efficient technology for quickly lowering the concentration of dissolved pollutants in an effluent. In this work, the hybrid process was applied for adsorption of Methyl Orange (MO) dye pollutant from simulated wastewater by using mesoporous MCM-41 as an efficient adsorbents coupling with a microfiltration membrane (MF) in a membrane adsorption reactor (MAR) system. Batch adsorption process has been achieved to investigate the effect of various parameters, such as; adsorbent dose, initial adsorbate concentration and contact time. The equilibrium adsorption data of MO onto MCM-41 were analyzed by Langmuir and Freundlich adsorption isotherms. Adsorption of MO by mesoporous material MCM-41 arrived at equilibrium in 20 min, and the system obeyed Langmuir isotherm model ($q_{\max} = 151.51$ mg/g), which is appropriate to monolayer adsorption. The kinetic pseudo-second order model appeared to match empirical datum completely. As for the hybrid process system (Mesoporous-MCM-41-MAR), the adsorption efficacy of MO and flux was 99% and 0.0006 ml/mm² min respectively, which was generally due to contribution of both systems at the same time, adsorption by mesoporous MCM-41 and filtration by membrane system. The hybrid process not only removed MO with high efficacy, but also actively separated and recycled mesoporous MCM-41.

Keywords: Membrane adsorption reactor (MAR); Hybrid system; Methyl orange; MCM41; Adsorption; Wastewater treatment

1. Introduction

Huge quantities of dyes are generated yearly and used in many industries, including the cosmetic, textile, leather, food, pharmaceutical and paper industries [1,2]. The existence of simple trace concentration of dyes in discharge is highly apparent and unwanted [3]. Colored wastewater causes aesthetic pollution and damages aquatic life [4]. Dye discharge commonly consists of chemicals, including the dye itself, which are toxic, mutagenic, carcinogenic, or teratogenic to various microbiological and fish species [5]. Methyl orange (MO) [C₁₄H₁₄N₃SO₃Na] is one of the most common of these dyes.

Low-pressure-driven membrane techniques such as ultrafiltration (UF) and microfiltration (MF) are considered necessary to remove particular pollutants from wastewater

that are not naturally removed by more traditional processes. UF and MF are superior in removing microorganisms, microparticles, colloids, macromolecules, and most bacteria. Membrane hybrid processes, such as membrane adsorption reactor (MAR) systems, are regarded as alternative methods to efficiently remove synthetic organic compounds (SOCs) and natural organic matter (NOM) in a cost-effective manner [6]. Hybrid or integrated membrane processes have been of interest for the last 20 years. Hybrid membrane processes can offer new, innovative solutions, and they offer new possibilities for sustainable industrial growth [7]. One of the biggest problems of membrane technology is membrane fouling, which can be targeted with hybrid membrane technologies. In practice, fouling reduces the permeate flux and can deteriorate the quality of permeate, therefore

decreasing membrane performance, i.e., productivity and membrane lifetime, and increasing the operating pressure (energy) needed. All these things increase the costs of water treatment [8]. In hybrid systems, other treatment technologies are used to obtain improved performance, including higher removal efficiency, an increased amount of treated water, a lower fouling tendency, etc. [7]. Most often, the term “hybrid processes” refers to the use of several different techniques one after another. The technologies combined may be conventional treatment technologies, such as precipitation, ion-exchange, adsorption, or other membrane technologies [9,10]. Some researchers are combining membrane processes with adsorption systems [11–13]. For example, Powell et al. [14] coupled activated carbon with a membrane process, and discovered that activated carbon has dual functions: membrane fouling control and virus adsorption. Zacaria et al. [15] investigated the lead and cadmium adsorption by a normal polysaccharide in an MF membrane reactor and concluded that the coupling of the adsorption step with an MF membrane was effective in limiting organic matter release and reserving adsorbent particles in the treated permeate. Nanoporous materials are much more effective than conventional adsorption materials because of their high adsorption capacity, small size, and large specific surface area. Furthermore, some nanoporous materials, and especially mesoporous materials such as SBA-15, MCM-48, and MCM-41, have excellent adsorption properties for wastewater treatment [16–20]. However, through conventional separation technologies such as sedimentation and flocculation, the nanoparticles are difficult to recycle and separate in wastewater treatment processes. This results in their secondary pollution of effluent and low rate of reuse. Combining membrane technology with mesoporous materials can effectively solve the problem [21].

The goal of the present research work is to improve a novel, effective and sustainable hybrid treatment process that simultaneously removes organic compounds such as MO dye from wastewater streams. The process is based on using membrane technology and adsorption process together, with mesoporous MCM-41 as adsorbent. The adsorption onto the surface MCM-41 is coupled with MF to test the efficacy of such a system in handling colored wastewater. The significance of operating parameters such as MCM-41 dosage and MO concentration on system performance are investigated by flux factor.

2. Materials and methods

2.1. Chemicals

Sodium hydroxide (NaOH), cetyltrimethylammonium bromide (CTAB, 99%), Tetraethyl orthosilicate (TEOS, 98%), ethanol (EtOH, 99%), and methyl orange (MO) [C₁₄H₁₄N₃SO₃Na] were purchased from Sigma Aldrich. The chemicals were used as received without additional purification.

2.2. Preparation of MCM-41 and characterization

The preparation of mesoporous MCM-41 as an adsorbent was achieved according to the traditional method [22].

The characterizations were also carried out on the adsorbent in our previous study [16].

2.3. Preparation of adsorbate solution

Adsorbate solution was prepared by dissolving 1 g of MO in 1,000 mL of deionized water in a conical flask, and then mixing for 2 h to make the MO particles fully dispersed in water. A calibration curve was then conducted from the methyl orange stock solution by using a UV-Spectrophotometer (HP 8453) set at 25°C. The λ max was found to be 464 nm. The calibration was fundamental to obtaining the comparison of final adsorbance to initial.

2.4. Adsorption experiments

The mesoporous MCM-41 was used to remove the MO from aqueous solution of simulated wastewater by the batch adsorption system. An amount of MCM-41 was added to 1 L of MO solution in a conical flask placed on a magnetic mixer with its temperature set to 25°C. The various studied parameters are: (I) adsorbent dosage: (0.2–0.6 g); (II) MO concentration: (30–60 mg/L); (III) contact time: (0–80 min). The adsorbent normally buffered solution pH at 4. The transmembrane pressure was kept at a constant 1 bar for the experiment. The percentage of removal (%R) of MO solution was calculated at the end of the adsorption process by equation:

$$\%R = \frac{C_0 - C_e}{C_0} \times 100\% \quad (1)$$

where C_0 (mg/L) is initial concentration of MO and C_e (mg/L) is equilibrium concentration of MO.

2.5. Adsorption isotherm model

The Langmuir linear equation is given by [23]:

$$\frac{C_{eq}}{q_e} = \frac{1}{q_m} C_{eq} + \frac{1}{K_L q_m} \quad (2)$$

where q_e is the equilibrium adsorption capacity of adsorbent (mg/g), q_m (mg/g) is the maximum adsorption capacity and K_L (L/mg) is adsorption energy.

The constants q_m and K_L can be determined from Eq. (2) by the linear slope of $\frac{C_{eq}}{q_e}$ vs. C_{eq} . The equilibrium parameter of dimensionless R_L is defined as [24]:

$$R_L = \frac{1}{1 + K_L C_0} \quad (3)$$

The isotherm is favorable if $R_L < 1$, unfavorable if $R_L > 1$, irreversible if $R_L = 0$, or linear if $R_L = 1$ [25]. The Freundlich linear equation is as follows [26,27]:

$$\ln q_e = \ln K_f + \frac{1}{n} \ln C_{eq} \quad (4)$$

where n and K_f are Freundlich constants of adsorption intensity and adsorption capacity respectively. Freundlich constant n is an exponent measuring adsorption intensity, or surface heterogeneity, whose value lies in the range 1–10 for favorable adsorption phenomenon. The values of n and K_f can be determined from Eq. (4) by the slope and intercept of the linear plot of $\ln q_e$ vs. $\ln C_{eq}$.

2.6. Adsorption kinetics

The adsorption rate is analyzed by two kinetic models, pseudo-first and second order, which are expressed by Eqs. (5) and (6) respectively.

$$\log(q_t - q_e) = \log q_e - \frac{k_{1ads}}{2.303} t \quad (5)$$

where k_{1ads} is the pseudo-first order adsorption rate constant in min^{-1} and q_t is the amount of adsorption at time t in mg/g . The value of k_{1ads} can be empirically estimated by the slope of linear plot $\log(q_t - q_e)$ vs. t [16].

$$\frac{t}{q_t} = \frac{1}{k_{2ads} q_e^2} + \left(\frac{1}{q_e}\right) t \quad (6)$$

where k_{2ads} is the pseudo-second order adsorption rate constant of g/mg-min . The value of $k_{2ads} q_e^2$ can be obtained from the intercept and slope of plotting t/q_t vs. t [28].

2.7. Membrane materials

A microfiltration membrane with a diameter 1.2 mm, pore size 0.20 μm and membrane area 0.005181 m^2 was applied in this research. The membrane was purchased, and the required size of membrane of was cut for the experiments. All membranes were conditioned before to being used by pre-soaking for 4 h in ethanol.

2.8. Coupling system

The MAR system was assembled using one kind of microfiltration (MF) hollow fiber membrane module and the reactor volume was 1 L as shown in Fig. 1. The concentration of MO (30–60 mg/L) was added into the water to emulate wastewater earnestly polluted with MO, and MCM-41 was added and mixed well. One pump was used to get persistent inlet and outlet. Transmembrane pressure (TMP) remained constant at 1 bar. The process outlet flowed directly back to the reactor when no there was no sampling. To keep suspension circulated through the module, it was pumped at the constant rate of 1 L/min. Stirring in the reactor was guaranteed by the recycled flow of the retentive stream. The samples were taken and centrifuged (4,000 rpm, 5 min) in order to investigate the contribution of MCM-41 on the removal of MO. The membrane adsorption reactor was introduced with MO solution at pH 4 by a peristaltic pump, and its flow rate was permanently equal to the permeate flux. The permeate flux decrease was monitored during time. Consequently, the membrane reactor always worked at constant volume.

2.9. Steady-state analysis of the hybrid system

In order to accurately determine how much MO was removed by the MAR, the hybrid system was continuously checked for 80 min. Transmembrane pressure across the membrane module was 1 bar, and the initial concentration of MO was 30 mg/L , pH = 4, rpm = 250 and temperature = 25°C based on a previous study [16]. As shown in Fig. 1, operation time made no significant difference on membrane flux, which means no significant pollution was created on the surface of the membrane within 80 min and removal of MO by this hybrid system was steady state.

3. Results and discussion

3.1. Adsorbent characterization

The structural and textural features of the mesoporous material were studied using scanning electron microscopy (SEM), X-ray diffraction (XRD), nitrogen adsorption-desorption (BET) surface area, and Fourier transformer infra-red (FTIR) in previous research [16], and the results are shown in Table 1.

3.2. Adsorption equilibrium

Different adsorbent dosages of MCM-41 (0.2, 0.4, 0.5, and 0.6 g) were added to the MAR process to examine the removal efficacy of 30 g/L MO by the coupling system in the adsorption experiment. The outcomes appeared under empirical condition, four dosages of MCM-41 reached adsorption

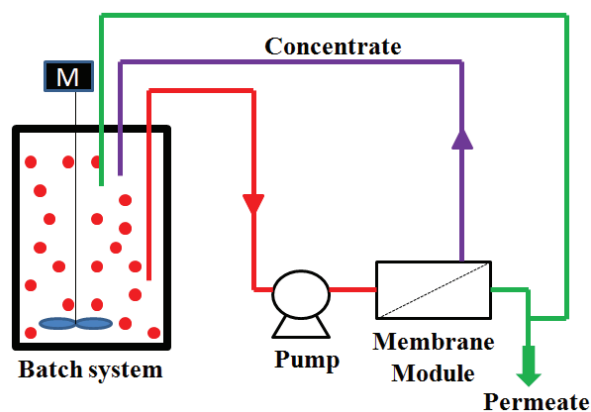


Fig. 1. Set-up of the adsorption-membrane reactor adsorption (MAR) system.

Table 1
Main characteristics of adsorbent MCM-41

Material	MCM-41
Average pore diameter DP (nm)	3.28
Pore wall thickness Wt (nm)	0.74
Total pore volume PV (cm^3/g)	0.94
Surface area S_{BET} (m^2/g)	1,450.9
Micro pore volume μ_p (cm^3/g)	0.132

equilibrium in around 20 min and removal exceeded 99%, as shown in Fig. 2. This was attributed to an increase in surface area of adsorption sites with the increased dosage of MCM-41, which thus enhanced the adsorption for MO, and because of the increase in total surface area. However, equilibrium adsorption capacity remained constant with increased initial dosage of MCM-41 [29]. That means adsorption capacity q_e is controlled by adsorption concentration C_e in solution and by adsorbent dosage. As a result, dosage of MCM-41 was used as 0.4 g in all experiments. It was indicated from this system and at the adsorbent dosage (0.4 g) of MCM-41; the removal efficiency factor obtained for MO using MCM-41 (99%) is higher than when powdered activated carbon modified by silver nanoparticles was used (72.5%) [30].

3.3. Adsorption isotherm

In this study, the two isotherm models, Langmuir and Freundlich adsorption isotherm, are applied to describe empirical data [14,31,32]. In the adsorption isotherm experiment, the initial concentrations of MO were set as 30, 40, 50, and 60 mg/l, the initial dose of MCM-41 was 0.5 g, and samples were taken after 80 min, as shown in Figs. 3 and 4 respectively.

3.3.1. Langmuir isotherm

The linear form of the Langmuir adsorption isotherm is given by Eq. (2). As shown in Fig. 3, uptake is increased with equilibrium concentration of MO in empirical concentration range. This is because of an increasing concentration gradient driving force. When concentration of MO is higher, the active sites of MCM-41 interact with more MO ions, and the system of adsorption increases. Therefore, values of q_e are increased with equilibrium concentrations of MO [33]. The linearized

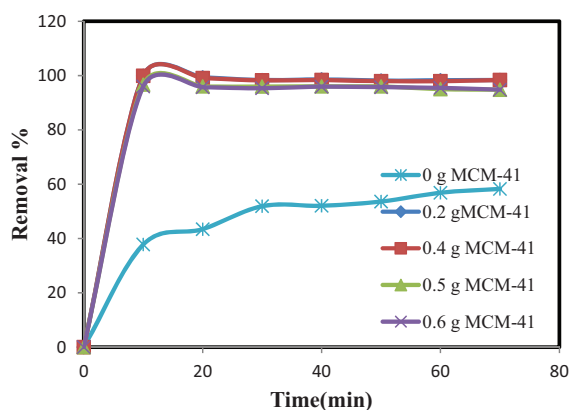


Fig. 2. Effect of contact time on removal of MO with different dosage of MCM-41.

Langmuir plot result is shown in Table 2, which gives the R^2 correlation coefficient and isotherm constants values. The correlation coefficient value for Langmuir isotherm of MCM-41 is 0.8374. The Langmuir isotherm fundamental feature may be expressed by the dimensionless constant called the separation factor (R_L) and is given by Eq. (3). R_L value is favorable between 0 and 1, which refers to adsorption of MO onto MCM-41, as shown in Table 2.

3.3.2. Freundlich isotherm

The Freundlich isotherm characterizes multilayer and physical adsorption over the heterogeneous surface [27]. According to the Freundlich isotherm, each adsorbing site has specific bond energy, stronger binding sites are occupied first, and adsorption energy decreases exponentially upon completion of process. The linear form of the Freundlich isotherm is given by Eq. (4). Both K_f and n predict the feasibility of the adsorption process. The linearized Freundlich plot is shown in Fig. 4, and the results are shown in Table 2, which gives the isotherm constants and R^2 correlation coefficient

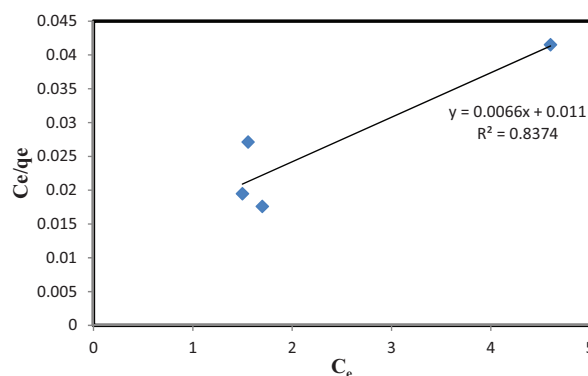


Fig. 3. Langmuir isotherm model.

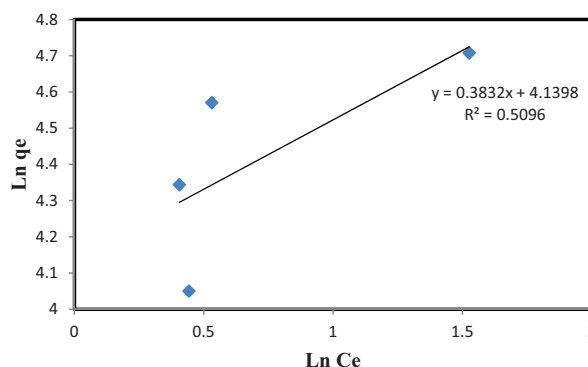


Fig. 4. Freundlich isotherm model.

Table 2
Isotherm models parameters

Adsorbent	Langmuir				Freundlich		
	q_{max} (mg/g)	K_L (L/mg)	R^2	R_L	K_F ($mg^{1-n} g^{-1} L^n$)	$1/n$	R^2
MCM-41	151.51	0.000073	0.8374	0.996	62.79	0.382	0.509

values. The value of the R^2 correlation coefficient for the Freundlich isotherm of MCM-41 is 0.5096. This value indicates that the Langmuir isotherm has a higher R^2 for MCM-41 than the Freundlich isotherm. It can be concluded that the adsorbent shows a good fit with empirical results [34]. Table 2 shows that a value of n less than 1 means poor adsorption characteristics, those in the range of 1–2 mean moderate adsorption, and 2–10 mean good [35]. The n value was 2.61; thus, the n value in the range of 1–10 provided information about favorability of MO adsorption onto MCM-41.

3.4. Kinetic study

The residence time for dye adsorption can be determined by kinetics examination of the equilibrium data. The kinetics of the MO adsorption onto MCM-41 from solution was inspected by two familiar kinetic models: pseudo-first and second order [28]. The non-linear forms of the two models are expressed by Eqs. (5) and (6). In this study, the initial concentration of MO was 30, 40, 50, and 60 mg/l, the dosage of MCM-41 was 0.5 g, and specimens were taken at 10, 20, 30, 40, 50, 60, and 70 min. Values of pseudo-first and second order rate constants and correlation coefficient are given in Table 3, and non-linear plots are shown in Figs. 5 and 6 respectively. The results indicate that among these two models, the pseudo-second order kinetic model had higher R^2 values and empirical q_e values that agree well with calculated q_2 values. The low R^2 for the pseudo-first order model indicates that this model did not suit the data well. Moreover, the empirical q_e was not in agreement with the calculated q_1 values. Consequently, the pseudo-second order kinetic model appears to be an excellent depiction of the MO adsorption mechanism [36].

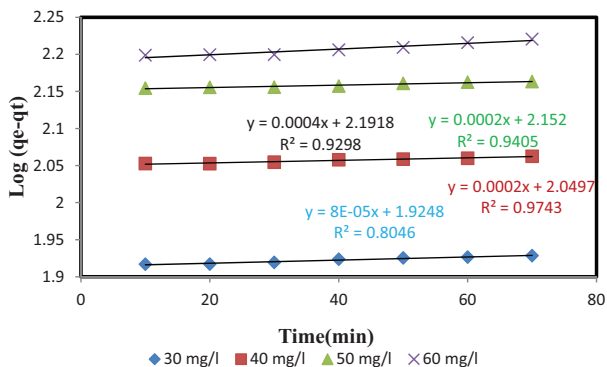


Fig. 5. Pseudo-first order kinetics model for MCM-41 at different concentration.

Table 3
Kinetic adsorption parameters by using Pseudo first and second order models

Concentration (mg/l)	q_e -exp (mg/g)	Pseudo-first-order			Pseudo-second-order		
		q_e -cal (mg/g)	k_1 (min ⁻¹)	R^2	q_e -cal (mg/g)	k_2 (g min ⁻¹ mg ⁻¹)	R^2
30	57.4	84.1	0.000184	0.8046	56.818	0.0143	0.9999
40	77	112.22	0.000461	0.9604	76.335	0.0286	0.9999
50	96.6	141.9	0.000461	0.9405	96.15	0.00092	0.9992
60	110.8	155.52	0.000921	0.9298	111.111	0.007788	0.9998

3.5. Removal of MO by the MCM-41 membrane coupling system

3.5.1. Effect of contact time on flux at different adsorbent dosages of MCM-41

The effect of adsorbent dosage of MCM-41 on flux permeates was tested by changing MCM-41 dosage while fixing initial dye concentration, pressure, and feed temperature. As shown in Fig. 7, the increase in adsorbent dosage from 0.2 to 0.6 g led to a slight decrease in permeates. However, varying the dosage beyond 0.2 g appeared to have small effect on the permeate flux of MO. This was expected because an increase in adsorbent dosage of MCM-41 would lead to more adsorption sites becoming available because of the high surface area of mesoporous material MCM-41, as listed in Table 1. Otherwise,

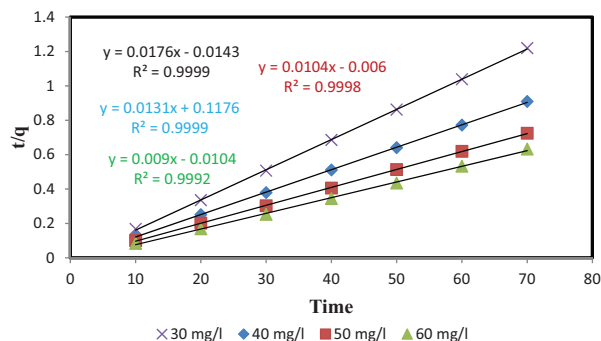


Fig. 6. Pseudo-second order kinetics model for MCM-41 at different concentration.

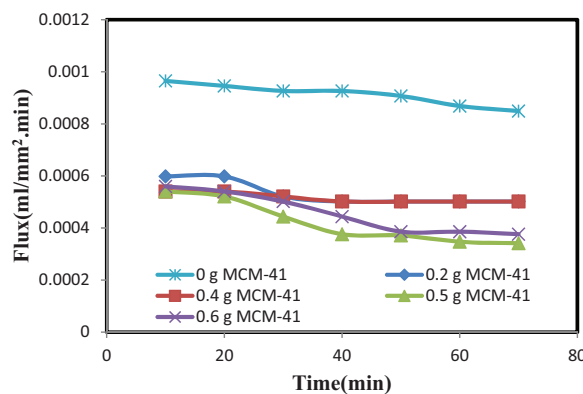


Fig. 7. Effect of contact time on flux at different dosage of MCM-41.

increasing adsorbent dosage increases the vacant number of adsorption sites vs. MO. These results correspond with adsorption literature concerning the influence of MCM-41 dosage on the removal of MO, where an increase in MCM-41 dosage led to a decrease in the remaining concentration of MO in solutions [16], even though permeate flux decreased as dosage of MCM-41 increased, as shown in Fig. 7. Permeate flux declined roughly 10% after increasing MCM-41 dosage from 0.2 to 0.6 mg. This behavior is anticipated, since increasing MCM-41 dosage in solution leads to increased strength between adsorbates and adsorbent become stronger, and the adsorption rates continuously increased [33].

3.5.2. Effect of contact time on flux at different concentration dosages of MO

The effect of contact time with changing concentrations of MO is an important parameter in MAR systems. The operating time effect on removal efficiency of MO and flux was investigated by changing MO concentration from 30–60 mg/l and using an adsorbent dosage of 0.5 g. Generally, if concentration polarization is not observed in the system, permeate flux remains fixed with time, as illustrated in Fig. 8. The flux decreased gradually with time at the four MO concentrations examined in this work. As mentioned previously, this indicates that the concentration polarization was influenced because the existence of MO in solution was significant. Actually, plots of high MO concentrations (50 and 60 mg/l) had sharper slopes than that of a low MO concentration (30 mg/l). This indicates that the resistance of suspended solids has greater significance at higher concentrations than lower ones. This result agrees with Al-Bastaki and Banat, 2004 [36]. From flux factor values, described in Fig. 8, it can be seen that increasing MO concentration, particularly at low MCM-41 dosage, may force some MCM-41 particles to collect at the membrane surface, creating another filtering layer. The significant layer became less influent as MO concentration was increased because of generation the concentration polarization layer [32].

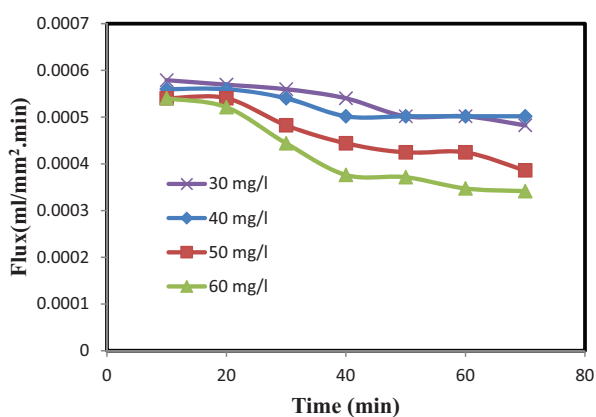


Fig. 8. Effect of contact time on flux with different concentration of MO.

4. Conclusion

The membrane adsorption hybrid system (MAHS) was efficient in removing dissolved MO from simulated wastewater. Adsorption by mesoporous material MCM-41 and filtration by (MF) membrane at the same time in a hybrid system was influenced both MO removal efficacy and flux improvement. The empirical data was successful in describing the adsorption of MO onto the MCM-41 as well as flux of the membrane adsorption system. The adsorption isotherm correlation coefficient (R^2) is an empirical parameter in the model. The higher R^2 value produced higher removal efficiency of MO. Adsorption of MO by nanoporous MCM-41 achieved equilibrium within 20 min, and it agreed with the Langmuir isothermal adsorption model. The pseudo-second order kinetic model depicts the adsorption process and adsorption of MO by nanoporous MCM-41 perfectly. The coupling of nanoporous MCM-41 and an MF membrane were increased the removal efficacy of MO and the interception efficacy of the MAR process. The adsorption of nanoporous MCM-41 and the cake layer, or concentration polarization, produced on the surface of the membrane made the hybrid process stable and efficient in removing MO. Industrial discharges commonly consist of suspended and dissolved matter. Therefore, the integration of MF and adsorption in one system allows for the removal of large molecules such as colloids by MF and of low-molecular-weight compounds like dyes by adsorption.

Acknowledgements

I thank the Department of Chemical Engineering, University of Technology, Baghdad, Iraq, for their scientific help and financial support.

References

- [1] V.V. Ranade, V.M. Bhandari, Industrial wastewater treatment, recycling, and reuse: an overview. In: V.V. Ranade, V.M. Bhandari, eds., *Industrial Wastewater Treatment, Recycling and Reuse*. Oxford, Butterworth-Heinemann Ltd: Chapter 1, 2014, pp. 1–80.
- [2] N.D. Lourenço, J.M. Novais, H.M. Pinheiro, Effect of some operational parameters on textile dye biodegradation in a sequential batch reactor, *J. Biotechnol.*, 89 (2001) 163–174.
- [3] O.J. Hao, H. Kim, P.C. Chiang, Decolorization of wastewater, *Crit. Rev. Environ. Sci. Technol.*, 30 (2000) 499–505.
- [4] A.H. Gemeay, I.A. Mansour, R.G. El-Sharkawy, A.B. Zaki, Kinetics and mechanism of the heterogeneous catalyzed oxidative degradation of indigo carmine, *J. Mol. Catal. A: Chem.*, 193 (2003) 109–120.
- [5] N. Daneshvar, H. Ashassi-Sorkhabi, A. Tizpar, Decolorization of orange II by electrocoagulation method, *Separ. Purif. Technol.*, 31 (2003) 153–162.
- [6] T. Lebeau, C. Lelièvre, H. Buisson, D. Cléret, L.W. Van de Venter, P. Côté, Immersed membrane filtration for the production of drinking water: combination with PAC for NOM and SOCs removal, *Desalination*, 117 (1998) 219–231.
- [7] G. Kang, Y. Cao, Development of antifouling reverse osmosis membranes for water treatment: a review. *Water. Res.*, 46 (2012) 584–600.
- [8] E. Drioli, A. Stankiewicz, F. Macedonio, Membrane engineering in process intensification An overview, *J. Membr. Sci.*, 380 (2011) 1–8.
- [9] A.I. Dalvi, M.N. Kither Mohammad, S. A1-Sulami, K. Sahul, R. A1-Rasheed, Effect of various forms of iron in recycle brine

- on performance of scale control additives in MSF desalination plants, *Desalination*, 123 (1999) 177–184.
- [10] W.L. Ang, A.W. Mohammad, A. Benamor, N. Hilal, Chitosan as natural coagulant in hybrid coagulation-nanofiltration membrane process for water treatment, *J. Env. Chem Eng.*, 4 (2016) 4857–4862.
- [11] R. Mirzajani, S. Ahmadi, R. Malakooti, H. Mahmoodi, Fast and efficient adsorption of azure (II) on nanoporous MCM-41 for its removal, preconcentration and determination in biological matrices, *J. Porous. Mater.*, 21 (2014) 413–421.
- [12] T.M. Albayati, A.A. Sabri, R.A. Alazawi, Separation of methylene blue as pollutant of water by SBA-15 in a fixed-bed column, *Arabian. J. Sci. Eng.*, 41 (2016) 2409–2415.
- [13] N. Kabay, M. Bryjak, S. Schlosser, M. Kitis, S. Avlonitis, Z. Matejka, I. Al-Mutaz, M. Yuksel, Adsorption-membrane filtration (AMF) hybrid process for boron removal from seawater: an overview, *Desalination*, 223 (2008) 38–48.
- [14] T. Powell, G.M. Brion, M. Jagtoyen, F. Derbyshire, Investigating the effect of carbon shape on virus adsorption, *Environ. Sci. Technol.*, 34 (2000) 2779–2783.
- [15] Z. Reddad, C. Gerente, Y. Andres, J.-F. Thibault, P. Le Cloirec, Cadmium and lead adsorption by a natural polysaccharide in MF membrane reactor: experimental analysis and modelling, *Water. Res.*, 37 (2003) 3983–3991.
- [16] T.M. Albayati, G.M. Alwan, O.S. Mahdy, High performance methyl orange capture on magnetic nanoporous MCM-41 prepared by incipient wetness impregnation method, *Korean. J. Chem. Eng.*, 34 (2017) 259–265.
- [17] A.A. Sabri, T.M. Albayati, R.A. Alazawi, Synthesis of ordered mesoporous SBA-15 and its adsorption of methylene blue, *Korean. J. Chem. Eng.*, 32 (2015) 1835–1841.
- [18] T.M. Albayati, A.M. Doyle, Shape-selective adsorption of substituted aniline pollutants from wastewater, *Adsorpt. Sci. Technol.*, 31 (2013) 459–468.
- [19] T.M. Albayati, A.M. Doyle, Purification of aniline and nitrosubstituted aniline contaminants from aqueous solution using beta zeolite, *Chemistry: Bulgar. J. Sci. Educ.*, 23 (2014) 105–114.
- [20] T.M. Al-Bayati, Removal of aniline and nitro-substituted aniline from wastewater by particulate nanoporous MCM-48, *Part. Sci. Technol.*, 32 (2014) 616–623.
- [21] R. Pelton, X. Geng, M. Brook, Photocatalytic paper from colloidal TiO₂ act or fantasy, *Adv. Colloid. Inter.*, 127 (2006) 43–53.
- [22] L. Chen, T. Horiuchi, T. Mori, K. Maeda, Post synthesis hydrothermal restructuring of M41S mesoporous molecular sieves in water, *J. Phys. Chem. B.*, 103 (1999) 1216–1222.
- [23] W.J. Weber, R.K. Chakravorti, Pore and solid diffusion models for fixed-bed adsorbers, *J. Am. Inst. Chem. Eng.*, 20 (1974) 228–238.
- [24] I. Langmuir, The constitution and fundamental properties of solids and liquids Part I. Solids, *J. Am. Chem. Soc.*, 38 (1916) 2221–2295.
- [25] M. Chen, Y. Chen, G.W. Diao, Adsorption kinetics and thermodynamics of methylene blue onto p-tert-butyl-calix [4,6,8] arene-bonded silica gel, *J. Chem. Eng. Data.*, 55 (2010) 5109–5116.
- [26] H.M. Freundlich, Colloid capillary chemistry, *J. Chem. Educ.*, 3 (1926) 1454–1455.
- [27] H.M. Freundlich, Uber die adsorption in lasugen, *J. Phys. Chem.*, 57A (1906) 385–470.
- [28] Y.S. Ho, G. McKay, Pseudo-second order model for sorption processes, *Process. Biochem.*, 34 (1999) 451–465.
- [29] T.C. Voice, W.J. Weber, Sorbent concentration effects in liquid/solid Partitioning, *Environ. Sci. Technol.*, 19 (1985) 789–796.
- [30] J. Pal, M.K. Deb, D.K. Deshmukh, D.Verma; Removal of methyl orange by activated carbon modified by silver nanoparticles, *Appl. Water. Sci.*, 3 (2013) 367–374.
- [31] V.S. Munagapati, V. Yarramuthi, D-S Kim, Methyl orange removal from aqueous solution using goethite, chitosan beads and goethite impregnated with chitosan beads, *J. Mol. Liq.*, 240 (2017) 329–339.
- [32] Z. Xiang, C. Di, W. Zhiwei, L. Yang, C. Rong, Nano-TiO₂ membrane adsorption reactor (MAR) for virus removal in drinking water, *Chem. Eng. J.*, 230 (2013) 180–187.
- [33] I. Langmuir, The adsorption of gases on plane surfaces of glass, mica and platinum, *J. Am. Chem. Soc.*, 40 (1918) 1361–1403.
- [34] T. Liu, Y. Li, Q. Du, J. Sun, Y. Jiao, G. Yang, Z. Wang, Y. Xia, W. Zhang, K. Wang, H. Zhu, D. Wu, Adsorption of methylene blue from aqueous solution by grapheme, *Colloids. Surf., B*, 90 (2012) 197–203.
- [35] Y. Yao, B. He, F. Xu, X. Chen, Equilibrium and kinetic studies of methyl orange adsorption on multiwalled carbon nanotubes, *Chem. Eng. J.*, 170 (2011) 82–89.
- [36] N. Al-Bastaki, F. Banat, Combining ultrafiltration and adsorption on bentonite in a one-step process for the treatment of colored waters, *Resour. Conserv. Recycl.*, 41 (2004) 103–113.